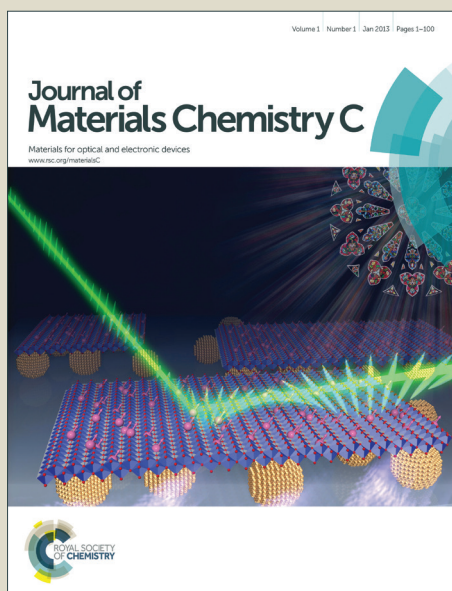


Journal of Materials Chemistry C

Accepted Manuscript



This article can be cited before page numbers have been issued, to do this please use: C. Y. Ang, S. Y. Tan, S. Wu, Q. Qu, M. F. E. Wong, Z. Luo, P. Li, S. Tamil Selvan and Y. Zhao, *J. Mater. Chem. C*, 2015, DOI: 10.1039/C5TC01465D.



This is an *Accepted Manuscript*, which has been through the Royal Society of Chemistry peer review process and has been accepted for publication.

Accepted Manuscripts are published online shortly after acceptance, before technical editing, formatting and proof reading. Using this free service, authors can make their results available to the community, in citable form, before we publish the edited article. We will replace this *Accepted Manuscript* with the edited and formatted *Advance Article* as soon as it is available.

You can find more information about *Accepted Manuscripts* in the [Information for Authors](#).

Please note that technical editing may introduce minor changes to the text and/or graphics, which may alter content. The journal's standard [Terms & Conditions](#) and the [Ethical guidelines](#) still apply. In no event shall the Royal Society of Chemistry be held responsible for any errors or omissions in this *Accepted Manuscript* or any consequences arising from the use of any information it contains.



Journal Name

ARTICLE

A Dual Responsive "Turn-On" Fluorophore for Orthogonal Selective Sensing of Biological Thiols and Hydrogen Peroxide

Chung Yen Ang,^{a,c,†} Si Yu Tan,^{a,†} Shaojue Wu,^a Qiuyu Qu,^a Mun Fei Eddy Wong,^a Zhong Luo,^a Pei-Zhou Li,^a Subramanian Tamil Selvan,^{c,d,*} and Yanli Zhao^{a,b,*}

Received 00th January 20xx,
Accepted 00th January 20xx

DOI: 10.1039/x0xx00000x

www.rsc.org/

Both of thiols and hydrogen peroxide (H₂O₂) have great correlations with cancer and other diseases, and hence the detection probes for sensing these agents may serve as early diagnostic tools. In this article, we report the development of a dual responsive probe that has the ability to generate two different responses upon reacting with thiols and H₂O₂ in a highly selective manner. The probe (FLB₂SSCou) consists of a coumarin unit and a diboron xanthene spiro isobenzofuran group bridged by a disulfide bond. The detection experiments show that the probe could selectively respond to thiols and H₂O₂ when screening a substrate library containing 20 amino acids, homocysteine, glutathione, dithiothreitol and H₂O₂. The initial off state of the probe was a result of photo-induced electron transfer (PET) from the coumarin group to non-fluorescing diboron xanthene spiro isobenzofuran group bridged by a disulfide bond. Reductive cleavage of the disulfide bond leads to the termination of this PET process, thus switching on the fluorescence of the probe. On the other hand, the oxidation of the diboron group by H₂O₂ converts the non-fluorescing group into highly fluorescing fluorescein group. Time-dependent density functional theory calculations were then performed to explain the PET process, and the obtained results indicate that the PET process occurs from the second excited state (S₂) into the first excited state (S₁). Finally, the imaging and detection experiments of the probe on HeLa cancer cells were conducted by means of fluorescence microscopy and flow cytometry technique. It was observed that the fluorescence of the FLB₂SSCou probe could be switched on by endogenous thiols and exogenous H₂O₂, demonstrating the applicability of this probe in both extracellular and intracellular environments. The present work exhibits a novel development of a dual responsive probe as contrast to commonly reported single responsive fluorescence probe, which may inspire future design of multiple responsive fluorescence probes.

Introduction

Stimuli-responsive fluorescence probes have received a great deal of attention on account of their special applications for sensing and imaging.¹⁻⁸ Fluorescence-based sensing is cheaper and more preferred technique over other methods, since their preparations are relatively easy and the sensing applications could be realized without the use of sophisticated instruments.⁹⁻¹⁴ Fluorescent probes exhibit interesting properties, which react with the species of interest in a chemoselective manner. Hence, these probes are carefully

integrated with designed functional groups that would only interact with the substrate to induce an intended reaction for the generation of highly fluorescent adducts. Recently, Liu *et al.* have reported a coumarin based fluorescence probe that has the ability to discriminate glutathione (GSH), cysteine (Cys) and homocysteine (Hcy) in a simultaneous fashion.¹⁵ In this work, the fluorescence probe reacts with these three biological thiol compounds differently and produces fluorescent adducts with different excitation and emission. Other than this work, there are various reported examples for highly selective detections of thiols by means of fluorescence technique.¹⁶⁻²⁸ However, dual-responsive fluorescence probes that can respond to two different types of analytes with different signals have not been commonly reported.

It is well known that the presence of high intracellular concentration of thiols has a great correlation with certain types of diseases.²⁹⁻³⁶ In particular, it was reported that the intracellular environment of most cancer cell lines expresses high concentration of GSH.³⁷⁻⁴¹ In view of this fact, various drug delivery systems were designed for GSH-triggered release of anticancer drugs within cancer cells.^{31,42-50} On the other hand, H₂O₂ was also reported as one of major reactive oxygen species (ROS) that are capable of inducing oxidative stress to

^a Division of Chemistry and Biological Chemistry, School of Physical and Mathematical Sciences, Nanyang Technological University, 21 Nanyang Link, 637371 Singapore. Email: zhaoyanli@ntu.edu.sg

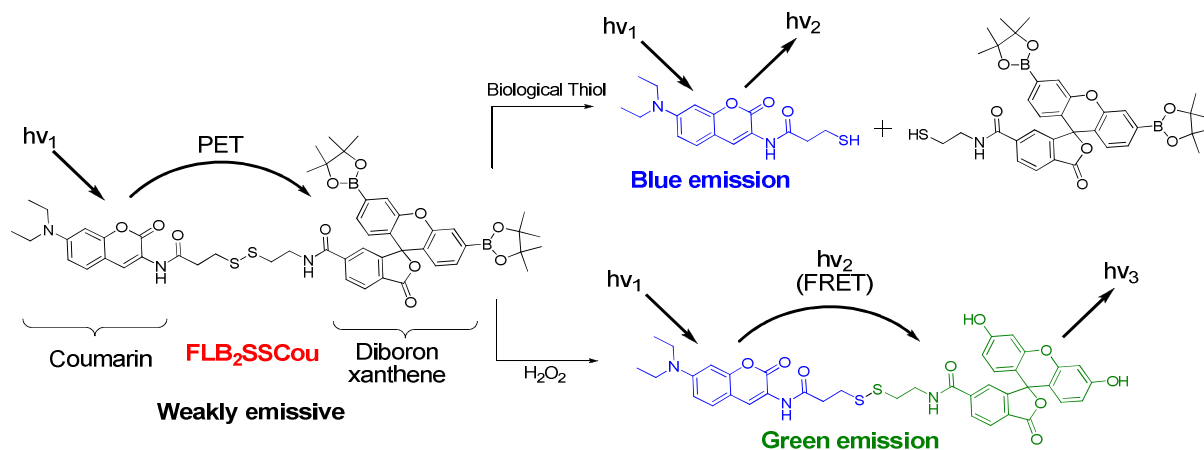
^b School of Materials Science and Engineering, Nanyang Technological University, 60 Nanyang Drive, 637551 Singapore.

^c Institute of Material Research and Engineering, 3 Research Link, Singapore 117602, Singapore. Email: subramaniant@imre.a-star.edu.sg

^d National University of Singapore, Division of Biomedical Engineering, Faculty of Engineering, 7 Engineering Drive 1, 117576 Singapore.

† These authors contributed equally to this work.

Electronic Supplementary Information (ESI) available: Additional synthesis and characterization data. See DOI: 10.1039/x0xx00000x



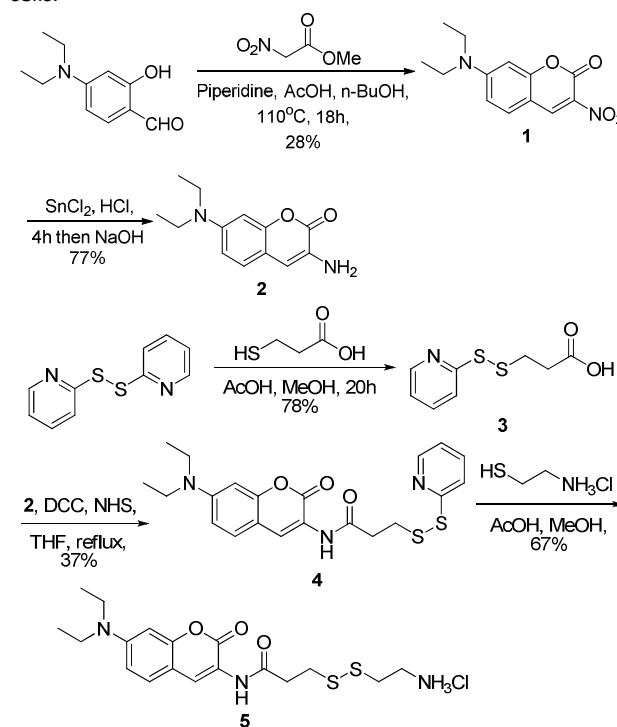
Scheme 1. Schematic illustration for the working mechanisms of dual responsive "turn-on" fluorescence probe FLB₂SSCou when interacting with biological thiols and H₂O₂.

physiological environment.⁵¹⁻⁵⁴ High concentration of physiological H₂O₂ was known to associate with various issues such as aging, cancer, Alzheimer's disease and cardiovascular disorder.⁵⁵⁻⁶¹

Herein, we designed a "turn-on" fluorescence probe that is not only responsive to biological thiol compounds and H₂O₂, but also capable of discriminating these two types of analytes in a highly selective manner by generating different responses. Moreover, this probe is able to detect these two types of analytes when they are present simultaneously in the intracellular environment.

The design of this "turn-on" probe was based upon a coumarin-containing group that was conjugated to a diboron xanthene spiro isobenzofuran bridged by a disulfide bond (FLB₂SSCou in Scheme 1). In the initial form, the probe would be in its dark state whereby the fluorescence of the coumarin is quenched by non-fluorescing diboron xanthene spiro isobenzofuran through the photo-induced electron transfer (PET) mechanism. The PET mechanism was supported by the absence of spectral overlapping between the absorption peak of diboron xanthene spiro isobenzofuran and the emission peak of coumarin. We thus ruled out the possibility of the Förster resonance energy transfer (FRET) between the two moieties in the dark state. Upon reaction with a biological reducing thiol, the disulfide bond would be cleaved and the coumarin unit is separated from diboron xanthene spiro isobenzofuran. This process terminates the electron transfer from coumarin to diboron xanthene spiro isobenzofuran, regaining the fluorescence from the coumarin moiety. When the probe reacts with H₂O₂, the diboron functional group on xanthene would be oxidized into corresponding fluorescein entity.⁶² This process converts the PET mechanism from coumarin into the FRET mechanism, thereby turning on green fluorescence under the same excitation of the coumarin moiety. This phenomenon is understandable, since coumarin/fluorescein is a common FRET pair reported in literature.⁶³⁻⁶⁶ Hence, the diboron xanthene spiro isobenzofuran group serves as not only a quencher for the coumarin group, but also a secondary probe.

With this design in mind, we conducted this work in a systematic manner, beginning with the synthesis of the probe, followed by the studies of its various optical properties, and finally proving the PET mechanism by utilizing the density functional theory (DFT). Thereafter, we proceeded to test the applicability of the probe for simultaneous imaging of intracellular thiol compounds and H₂O₂ in live HeLa cancer cells.

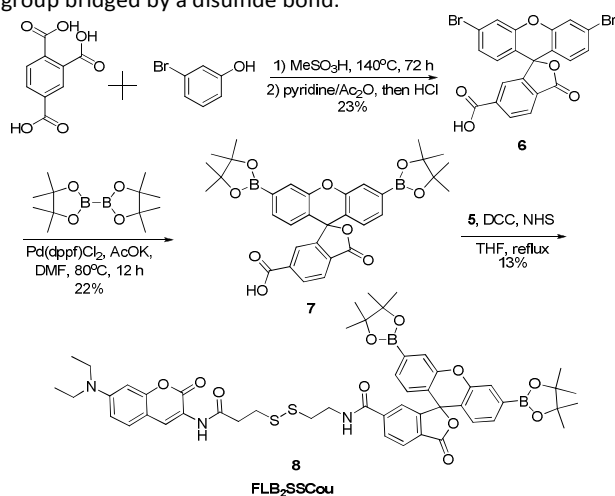


DCC = dicyclohexylcarbodiimide, NHS = N-hydroxysuccinimide
Scheme 2. Synthetic scheme for coupling a disulfide bond with a coumarin unit.

Results and discussion

Synthesis of FLB₂SSCou. The synthesis of the FLB₂SSCou probe was accomplished in a total of 8 synthetic steps (Schemes 2

and 3). The synthetic strategy begins with the preparation of 7-diethylamino-3-aminocoumarin (**2**) from 4-diethylsalicylihyde through two-step reactions. Firstly, 4-diethylsalicylihyde reacted with methyl-2-nitroacetate to afford a coumarin compound (**1**) by a Knoevenager condensation using piperidine as the amine catalyst in the presence of acetic acid. Thereafter, the nitro group on compound **1** was reduced to corresponding amino group on compound **2** in a good yield. The amino group of resulted compound **2** was functionalized with an activated thiol by reacting with 3-(pyridin-2-yl-disulfanyl)propanoic acid (**3**) through dicyclohexylcarbodiimide (DCC) / N-hydroxysuccinimide (NHS) coupling, affording compound **4**. With the availability of a pyridin-2-yl-disulfanyl group on compound **4**, it can easily react with the thiol group of 2-mercaptoethanamine hydrochloride to afford compound **5**. Thus, compound **5** contains a coumarin moiety and an amino group bridged by a disulfide bond.



Scheme 3. Synthesis of H_2O_2 responsive diboron xanthene spiro isobenzofuran precursor and FLB_2SSCou probe.

In order to obtain H_2O_2 responsive diboron xanthene spiro isobenzofuran unit of the probe, we adopted a two-step synthetic procedure (Scheme 3).⁶⁷ It was reported that the diboron group in molecular probes has the ability to react with H_2O_2 in a highly selective manner through oxidative deprotection of the boronic ester group.^{64,68-77} Thus, it was expected that the introduction of the diboron unit could endow the highly selective detection of H_2O_2 into the dual responsive probe.⁶⁸ In the synthesis, 2 equivalents of benzene-1,2,4-tricarboxylic acid condensed with one equivalent of 3-bromophenol to form the dibromo xanthene spiro isobenzofuran derivative **6**. Due to unsymmetrical nature of benzene-1,2,4-tricarboxylic acid, the crude product consisted of a mixture of two isomers in which the carboxylic acid unit was on either 5- or 6-position of the isobenzofuran site. Based on the reported procedure, the isomer with carboxylic acid on the 6-position was isolated by salting out as a pyridine salt in acetic anhydride/pyridine mixture. Thereafter, the pyridine salt was neutralized back into the carboxylic acid group. The two bromine groups on the xanthene moiety in compound **6** were then converted into the pinacolato boronic esters by

palladium mediated coupling reaction with bis(pinacolato)diboron, affording compound **7**. Finally, the carboxylic acid group on compound **7** was used as the coupling site with compound **5** to achieve the target probe **8** (or FLB_2SSCou).

Spectroscopic properties and optical responses of FLB_2SSCou toward H_2O_2 and biological thiols. After obtaining FLB_2SSCou , we performed a series of optical studies of this molecule to investigate its response toward biological thiols and H_2O_2 . We first measured the absorption spectra of FLB_2SSCou before and after the introduction of 1.0 mM H_2O_2 and 5.0 mM dithiothreitol (DTT), respectively (Figure 1A). It was observed that all the absorption spectra exhibited a common maximum peak at the wavelength of 408 nm. However, the absorption spectrum of FLB_2SSCou after the reaction with H_2O_2 showed a new signal at 497 nm. This new absorption peak coincides with typical absorption signal of a fluorescein molecule, indicating that the oxidation of the two boronic acid units on diboron xanthene spiro isobenzofuran indeed produced corresponding fluorescein moiety.

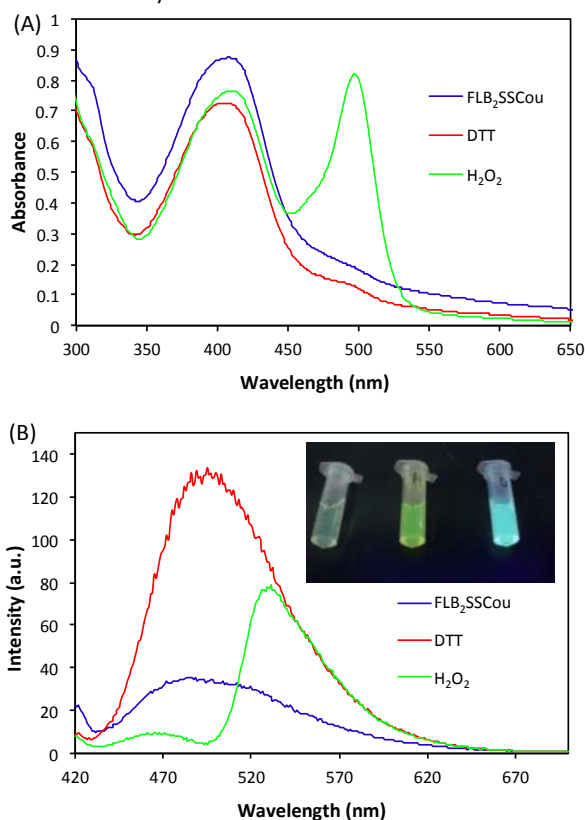


Fig 1. (A) UV-Vis and (B) fluorescence spectra of FLB_2SSCou (50 μM) in the absence and presence of H_2O_2 (1.0 mM) or DTT (5.0 mM) after overnight incubation at 37 $^\circ\text{C}$. Fluorescence spectra were measured under the excitation wavelength of 408 nm. Inset of Fig 1B shows photoluminescence images of the three samples upon irradiation at 365 nm by a handheld UV lamp. Images from left to right are FLB_2SSCou , FLB_2SSCou after treatment with H_2O_2 , and FLB_2SSCou after treatment with DTT.

We next performed the fluorescence measurements of FLB_2SSCou before and after the DTT and H_2O_2 treatments (Figure 1B). The probe without any treatment exhibited a weak

ARTICLE

Journal Name

fluorescence peak at 497 nm ($\Phi = 0.001$). Upon the treatment with DTT, the fluorescence intensity enhanced at the same wavelength of 497 nm ($\Phi = 0.168$). On the other hand, when the probe was treated with H_2O_2 , it showed a fluorescence enhancement at 525 nm and a fluorescence decrease at 497 nm ($\Phi = 0.101$). As abovementioned, the treatment of the probe with H_2O_2 led to the emergence of a new absorption peak at 497 nm. Thus, a complete spectral overlapping occurs between the emission of coumarin unit at 497 nm and the absorbance of the fluorescein moiety at 497 nm. This observation indicates that there is an FRET in the probe upon the treatment with H_2O_2 . The photographs in the inset of Figure 1B are the luminescence images of the probe upon excitation at 365 nm by a UV lamp before and after the DTT or H_2O_2 treatment. Distinctive difference in the fluorescence color between the three samples was observed, thus confirming that the probe indeed possesses the capability to show different responses upon the treatment with thiols and H_2O_2 .

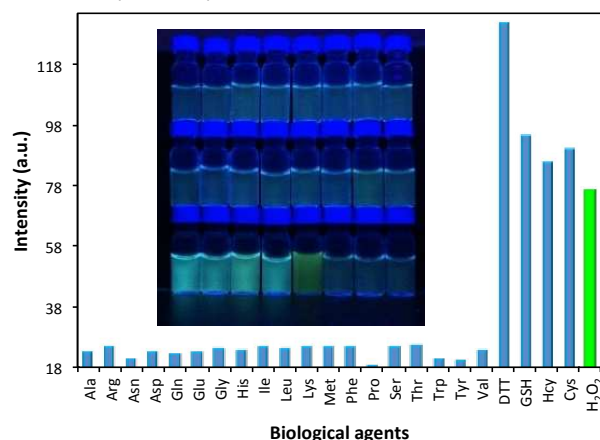


Fig 2. Fluorescence responses of FLB₂SSCou (50 μ M) toward various amino acids (5.0 mM), biological thiols (5.0 mM), and H_2O_2 (1.0 mM). All emission spectra were measured under the excitation of 408 nm, and the value of the emission intensity was obtained at the wavelength of 497 nm (except for H_2O_2). The emission intensity for H_2O_2 was obtained at the wavelength of 525 nm. Inset: Fluorescence images of the FLB₂SSCou solution after the addition of various additives upon excitation at 365 nm by a handheld UV lamp. Images from bottom left to top right are for: DTT, GSH, Hcy, Cys, H_2O_2 , Ala, Arg, Asn, Asp, Gln, Glu, Gly, His, Ile, Leu, Lys, Met, Phe, Pro, Ser, Thr, Trp, and Val.

We also studied the responsivity of the probe toward thiol (DTT) and H_2O_2 in acidic condition by measuring time dependent fluorescence response (Figure S1 in ESI). When comparing the fluorescence responsivity of FLB₂SSCou to DTT in pH 7.4 and 5.5, it was observed that the probe exhibits faster response to DTT in pH 7.4 than that in pH 5.5, which may be due to the presence of higher percentage of protonated thiol group on DTT in pH 5.5 than in pH 7.4. The protonation of the thiol group on DTT in acidic condition could decrease its nucleophilicity, and thus has a negative effect in reducing the disulfide bond of the probe. Interestingly, a different trend was observed when comparing the responsivity of the probe toward H_2O_2 in both pH conditions. Within the first 10 mins, there was higher responsivity of the probe to H_2O_2 in pH 7.4. Then, the rate decreased as compared to the

case in pH 5.5. Similar to the thiol-responsive mechanism, higher pH could induce the deprotonation of H_2O_2 and thus increase the initial response rate. On the other hand, lower pH could increase the hydrolysis rate of the borate group into corresponding hydroxyl group after the oxidation occurs. This explained the unexpected increment in the response rate of the probe to H_2O_2 in pH 5.5.

Selectivity and sensitivity studies. Primary advantage of the fluorescence probe is its dual responsive property and its capability of discriminating reducing thiols and oxidizing H_2O_2 . It is hence important to evaluate the selectivity and sensitivity of this probe toward biological thiols and H_2O_2 . Figure 2 shows the fluorescence responses of FLB₂SSCou upon treatments with various biological agents. As expected, FLB₂SSCou showed positive responses to DTT, GSH, Hcy, Cys and H_2O_2 only, whereas the rest of the amino acids did not induce any significant responses. Moreover, H_2O_2 exhibited a different response as compared with DTT, GSH, Hcy and Cys. This set of experiments confirmed that only thiol-containing biological agents have the ability to react with FLB₂SSCou by inducing a reductive cleavage of the disulfide bond to enhance the coumarin fluorescence. On the other hand, H_2O_2 can trigger a different response upon the reaction with FLB₂SSCou by oxidative deprotection of the boronic ester group into a highly fluorescent fluorescein derivative. It could be concluded that the probe has the capability to sense biological thiols and H_2O_2 without compromising its selectivity.

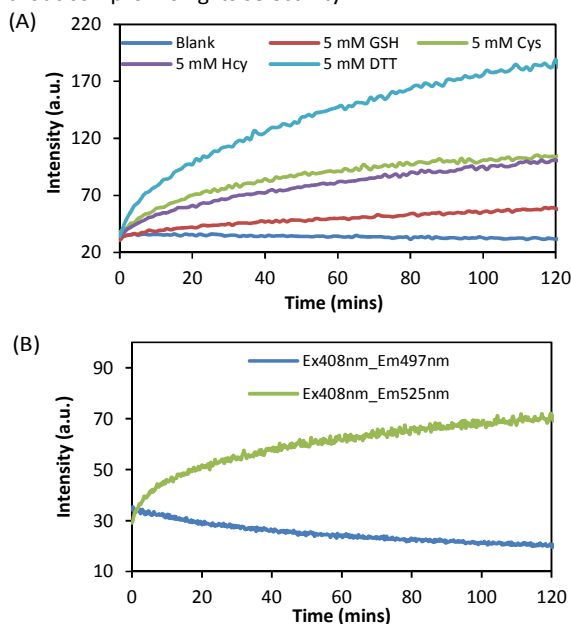


Fig 3. Time dependent fluorescence response of FLB₂SSCou (50 μ M) (A) in the absence (Blank) and presence of various biological thiol compounds (5.0 mM) as well as (B) by co-incubation with H_2O_2 (1.0 mM). Emission intensity in (A) was obtained at the wavelength of 497 nm under the excitation wavelength of 408 nm. Emission intensity in (B) was obtained at the wavelengths of 497 and 525 nm under the excitation wavelength of 408 nm.

We then studied the sensitivity of the probe toward H_2O_2 and biological thiols. Time-dependent optical responses of the probe to these agents were performed first. The experiments

were conducted by the co-incubation of FLB₂SSCOu (50 μM) and individual biological agent before measuring the emission spectra in a time-dependent basis under the excitation wavelength of 408 nm over a period of 120 min (Figure S2 in ESI). As a control, we also performed similar time-dependent fluorescence measurement of FLB₂SSCOu in the absence of any biological agent.

The real time fluorescence measurements of FLB₂SSCOu (50 μM) in the presence of various biological agents (Figure 3A) showed that DTT could induce the fastest and highest response rate as compared to other biological agents, reaching the fluorescence intensity approximately 6 times of higher than the starting fluorescence. Cys and Hcy were the second ones with similar response rate. GSH exhibited the slowest rate as compared to DTT, Cys, and Hcy. This is probably due to larger molecular weight of GSH, and hence, GSH would tend to induce higher activation energy during the reaction with the disulfide bond of the fluorescence probe as compared to smaller biological thiols.

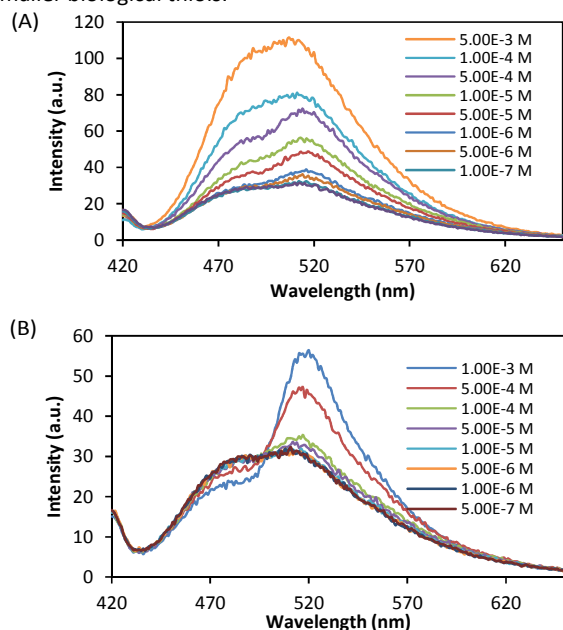


Fig 4. Changes in emission spectra of FLB₂SSCOu (50 μM) upon treatment with different amounts of (A) GSH and (B) H₂O₂ under the excitation wavelength of 408 nm.

In the presence of H₂O₂ (Figure 3B), FLB₂SSCOu showed the fluorescence signals at 497 nm and 525 nm under the excitation wavelength of 408 nm. It was found that the emission intensity at 497 nm decreased continuously, whereas the emission intensity at 525 nm increased correspondingly. This observation is in line with the result obtained from the

fluorescence spectra of FLB₂SSCOu upon treating with H₂O₂ (Figure 1B). From these observations, it could be further confirmed that the FRET process is indeed present between the coumarin moiety and the fluorescein group on the probe after the reaction with H₂O₂. The time dependent decreases in the emission signal at 497 nm correspond to the time dependent increases in the emission signal at 525 nm, due to the energy transfer upon the “turn-on” effect. This hence explained the similarity in the rate changes of the two emission intensities.

After performing these measurements, the response of the probe under different concentrations of GSH and H₂O₂ was investigated (Figure 4). The probe showed a good linear response toward GSH and H₂O₂ at the concentration ranges from 0.1 to 100 μM and 0.1 to 500 μM, respectively. Based on the linearity within the ranges, we computed the detection limits of the probe for GSH and H₂O₂ to be 4.98×10^{-6} M and 1.37×10^{-5} M, respectively. The relatively high detection limit of H₂O₂ could be attributed to the loss in the efficiency during the FRET process from the coumarin group to the fluorescein moiety. Note that the excitation wavelength used for the detection of H₂O₂ remained the same as the coumarin case at 408 nm instead of the direct excitation at 497 nm.

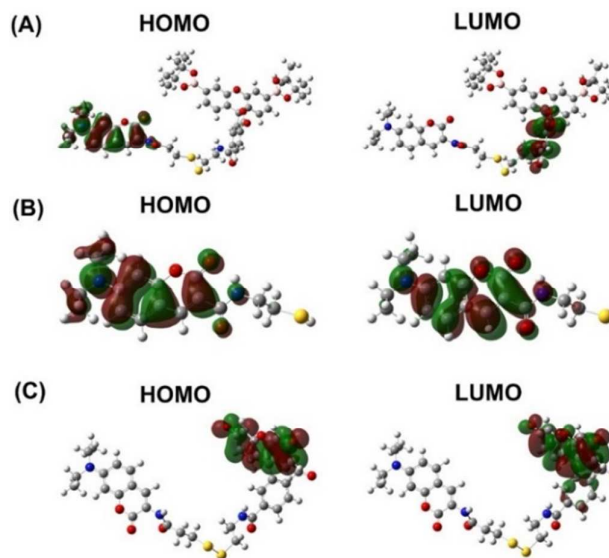


Fig 5. Calculated frontier molecular orbitals of (A) FLB₂SSCOu, (B) FLB₂SSCOu after reacting with thiols, resulting in the reductive cleavage of the disulfide bond to give a coumarin derivative, and (C) FLB₂SSCOu after reacting with H₂O₂, resulting in the oxidation of the boronic group into the phenoxy group.

Table 1. TD-DFT/B3LYP/6-31+G(d,p) calculation results of FLB₂SSCOu, FLB₂SSCOu treated with thiol, and FLB₂SSCOu treated with H₂O₂.

Molecule	Electronic transition ^a	Excitation wavelength (nm)	<i>f</i> ^b	Contributed orbitals	CI coefficient
FLB ₂ SSCOu	S ₀ → S ₁	394.02	0.0000	HOMO → LUMO	0.70704
	S ₀ → S ₂	377.44 (408)	0.6912	HOMO → LUMO + 1	0.70002
FLB ₂ SSCOu + Thiol	S ₀ → S ₁	388.58 (408)	0.8414	HOMO → LUMO	0.70089
FLB ₂ SSCOu + H ₂ O ₂	S ₀ → S ₁	447.77 (497)	0.7204	HOMO → LUMO	0.69911

^aDisplay of selected transition. ^bOscillator strength.

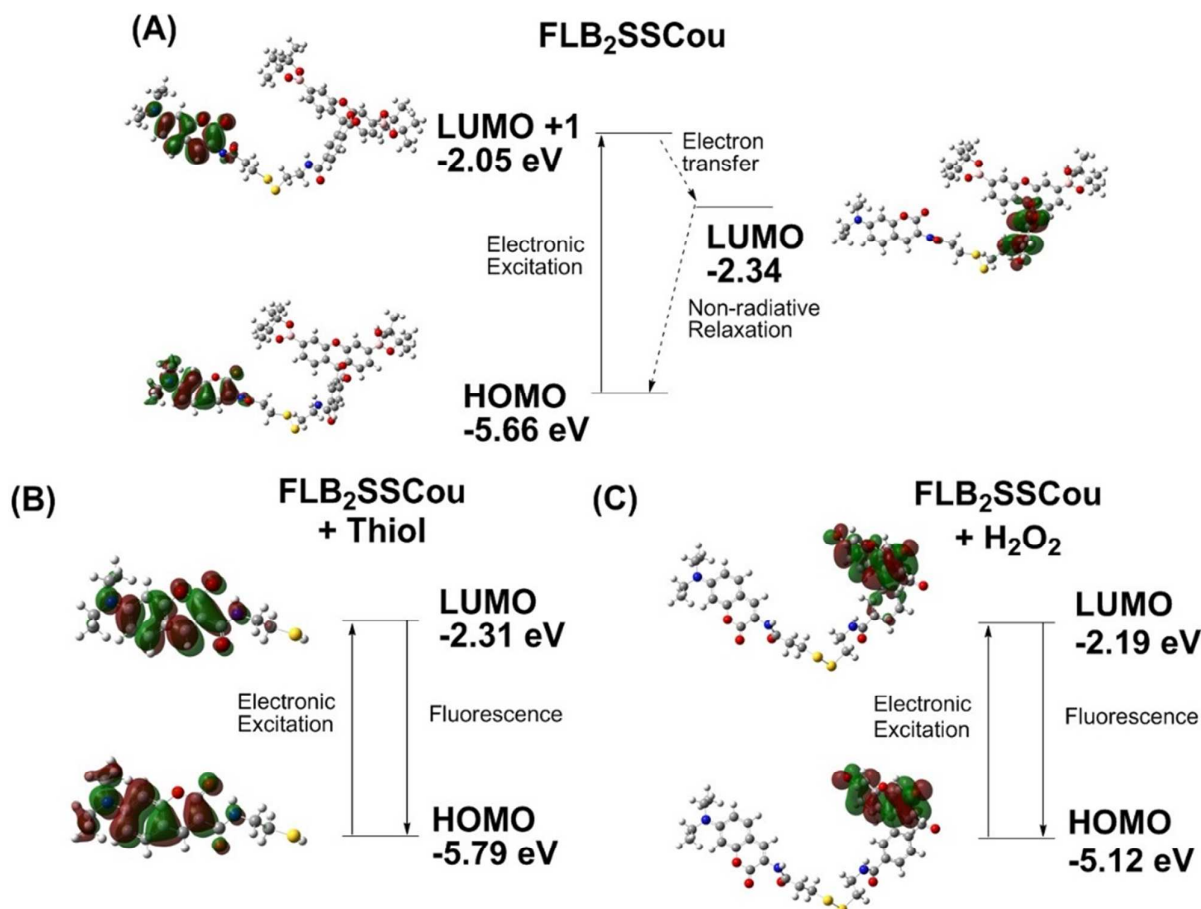


Fig 6. Energy level diagrams of (A) FLB₂SSCou, (B) FLB₂SSCou treated with thiol, and (C) FLB₂SSCou treated with H₂O₂, showing the electronic excitation as well as radiative and non-radiative relaxation pathways.

Computation studies. Based on experimental observations, it was speculated that the fluorescence of the initial dark state of FLB₂SSCou was quenched by the PET mechanism from the coumarin moiety to the diboron xanthene spiro isobenzofuran group. To confirm the existence of the PET phenomenon within the FLB₂SSCou probe, computational calculations on the molecule orbital locations were performed for the ground state and excited state. The ground state density functional theory (DFT) optimization of FLB₂SSCou in aqueous environment was first carried out at B3LYP/6-31+G(d,p) basis set using Gaussian 09 package.⁷⁸ Prior to the reaction with thiol compounds or H₂O₂, it was observed that the diboron xanthene group adopted spiro conformation with respect to the isobenzofuran group having the lactone ring intact in its close confirmation. The same optimization calculations on the probe upon the oxidative reaction with H₂O₂ were then performed. Since the reaction was conducted in neutral conditions, it was expected that the fluorescein group exists in the dianionic state during the calculation process. After the optimization process, we observed that the fluorescein group remained its spiro conformation, while the lactone ring was broken into the benzoic derivative. It was well documented that open ring form of fluorescein would exhibit high photoluminescence efficiency, whereas the lactone ring form shows no or weak fluorescence.⁷⁹⁻⁸¹

Thereafter, we performed time dependent-DFT (TD-DFT) calculation with the same basis set on the excited state in order to have better understanding of electronic transition pathway during the excitation. The same DFT optimization and TD-DFT calculation were also performed on the molecule after treatment with H₂O₂ and thiol compounds. The TD-DFT calculation results showed a lot of useful information, including calculated excited wavelength and oscillator strength (*f*) together with corresponding contributing orbitals (Table 1). Base on Kasha law, the fluorescence process is a result of direct relaxation from the 1st excited state (S₁) to the ground state (S₀).^{82, 83} Hence, we paid our attention to the first excited state of FLB₂SSCou before and after reacting with thiols and H₂O₂ from the TD-DFT calculation. It was observed that the electronic transition to the first excited state was mainly contributed from respective highest occupied molecular orbital (HOMO) to lowest unoccupied molecular orbital (LUMO) transition. Base on this information, we extracted the HOMO and LUMO orbital diagrams of these systems (Figure 5). After a careful examination of the transition, it was found that the S₀ to S₁ transition for FLB₂SSCou was accompanied by the oscillator strength of *f* = 0. This means that the direct excitation from its ground state to its first excited state is forbidden. The extracted HOMO and LUMO orbital diagrams of this molecule reveal that there is a re-distribution in its

electronic density from the coumarin group to the isobenzofuran group during this transition (Figure 5A). We observed that the lowest allowed transition lies on S_0 to the 2nd excited state (S_2) transition with an oscillator strength of $f = 0.6912$. For the cases of FLB₂SSCou after reacting with thiols and H₂O₂, the S_0 to S_1 transition accompanied by a non-zero f value provides a clear indication that the transition is an allowed process. The TD-DFT calculation results demonstrate that these transitions are contributed by the HOMO to LUMO transition, and a detailed observation on the orbital diagram shows no re-distribution of the electronic density during this HOMO to LUMO transition (Figure 5B and 5C). Based on these observations, we sketched out the orbital energy levels to explain the detailed mechanism of the “turn-on” effect (Figure 6).

From the TD-DFT calculation (Figure 6A), we can conclude that the photo-excitation of FLB₂SSCou induces an allowed electron excitation from the HOMO (-5.66 eV) to LUMO + 1 (-2.05 eV) orbitals ($S_0 \rightarrow S_2$, $f = 0.6912$), where there is no re-distribution of the electronic density. Thereafter, the excited electron is transferred to the LUMO (-2.34 eV) of the molecule with a net loss of 0.29 eV worth of energy. The electron transfer process is evident from the re-distribution of the electron density from the coumarin moiety to the isobenzofuran group on the orbital diagrams. The electron is then re-transferred back to the coumarin group by means of internal conversion, which is non-radiative in nature. This complete PET cycle explains the initial dark state of the molecule. By applying the same method of analysis to the molecule after the reductive cleavage of the disulfide bond and the oxidation of the diboron group into the phenoxide

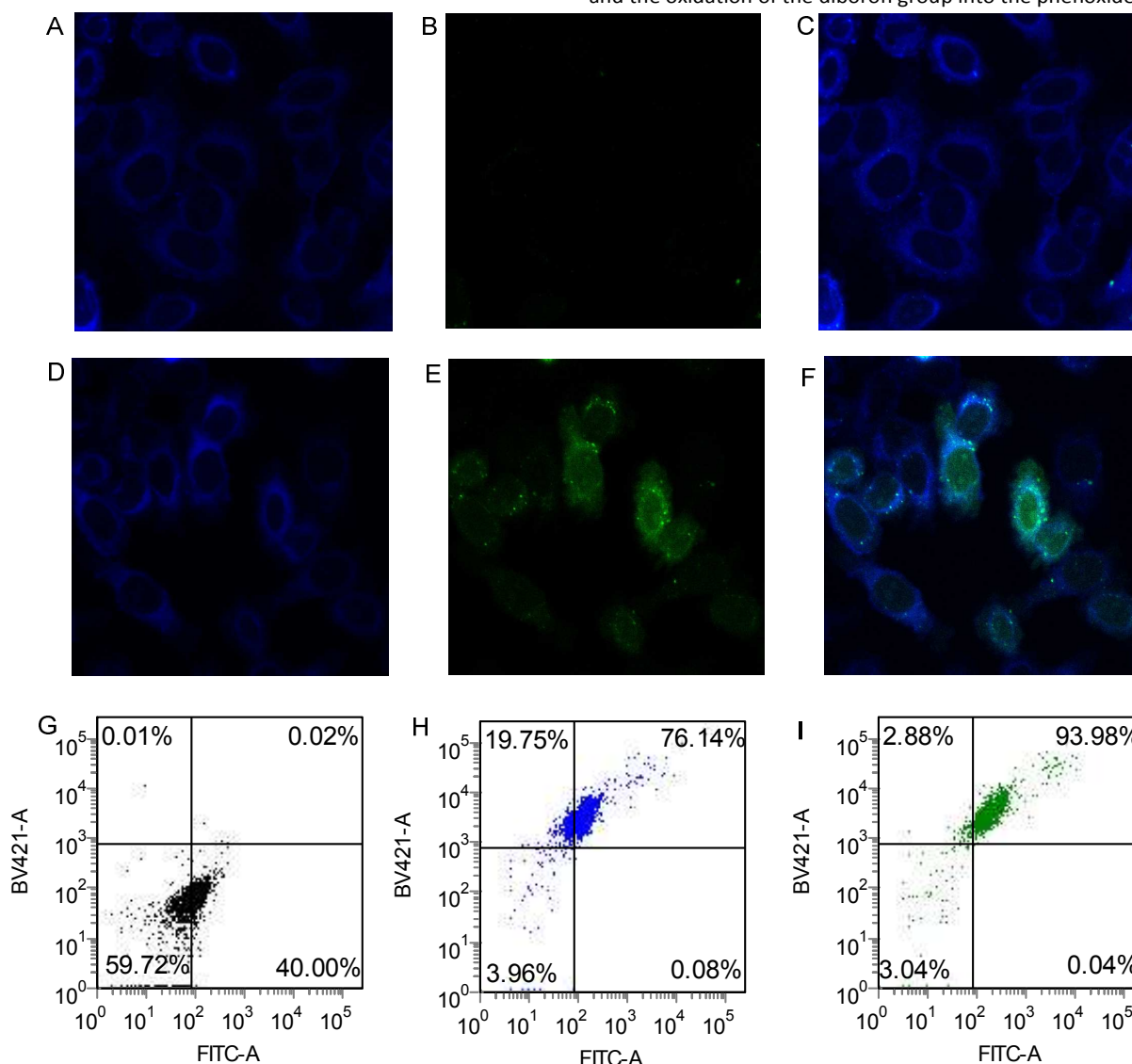


Fig 7. *In vitro* bioimaging of HeLa cells. Confocal scanning microscopic images of cells treated with 10 μM FLB₂SSCou and 20 μM β-CD under (A) 4',6-diamidino-2-phenylindole (DAPI) channel and (B) FITC channel. (C) Merged image of A and B. Confocal scanning microscopic images of cells treated with 10 μM FLB₂SSCou and 20 μM β-CD followed by post-treatment with 100 μM H₂O₂ under (D) DAPI channel and (E) FITC channel. (F) Merged image of D and E. Flow cytometry dot-plot diagram of HeLa cells (G) without any additives (blank control), (H) after treated with 10 μM FLB₂SSCou and 20 μM β-CD, and (I) after treated with 10 μM FLB₂SSCou and 20 μM β-CD followed by post-treatment with 150 μM H₂O₂.

group, chemically induced “turn-on” effect of FLB₂SSCou could be well explained. As seen from Figure 6B, the direct transition from HOMO to LUMO leads to no re-distribution in the electron density. Based on Kasha law, the absence of any intermediate orbital between S₁ and S₀ states confirms that the LUMO to HOMO relaxation is emissive. Similarly, we also did not observe any sign of PET from Figure 6C, thus concluding the conversion of the emissive FLB₂SSCou into two emissive adducts by terminating the PET process.

In vitro intracellular imaging of thiols and H₂O₂. In order to evaluate the applicability of the FLB₂SSCou probe for biological applications, we conducted the imaging of thiols and H₂O₂ in intracellular environment. Since it was well documented that most cancer cells possess high concentration of intracellular GSH, HeLa cells as the cancer cell model were selected in the studies. The biocompatibility of FLB₂SSCou was first evaluated using the 3-(4,5-dimethylthiazol-2-yl)-2,5-diphenyltetrazolium bromide (MTT) assay. The cell viability results showed that FLB₂SSCou exhibited insignificant toxicity to the cells (Figure S3 in ESI), making it suitable for subsequent biological applications. Intracellular imaging using FLB₂SSCou was then carried out. In this case, the pre-seeded cells were treated with FLB₂SSCou (10 μM) and β-cyclodextrin (β-CD, 20 μM) for 24 h prior to the imaging experiments. β-CD used was to facilitate the internalization of the probe. Based on the confocal scanning microscopy images (Figure 7A-7C), strong blue fluorescence from the cells was observed accompanied by some negligible green fluorescence signals.

The applicability of FLB₂SSCou for the imaging of intracellular H₂O₂ was then evaluated. Similarly, the pre-seeded HeLa cells were treated with FLB₂SSCou (10 μM) and β-CD (20 μM) for 24 h before the post-treatment of H₂O₂ for 45 min. As compared to previous images, a great increment in the green fluorescence of the cells under fluorescein isothiocyanate (FITC) channel (Figure 7D-7F) was observed. In addition, similar blue fluorescence intensity from the cells with and without the treatment with H₂O₂ was shown. According to the fluorescence studies, it was concluded that the treatment of FLB₂SSCou with H₂O₂ resulted in the emergence of a fluorescence signal at 525 nm (green emission) accompanied by the quenching of the blue emission due to the FRET mechanism. The spectroscopic observations seem different to the *in vitro* imaging results that the blue fluorescence remained the same for the cells with and without the post-treatment of H₂O₂. As observed from the UV-Vis studies, the treatment of FLB₂SSCou with H₂O₂ led to the emergence of a new absorption signal at 497 nm, which overlapped with the emission of coumarin unit at 497 nm. The presence of the disulfide bridge within the molecule allows the FRET process to occur especially when the distance between the FRET donor (coumarin) and the FRET acceptor (fluorescein) is not longer than 10 nm. Since both GSH and H₂O₂ exist in the intracellular environment, thiol-induced reductive cleavage of the disulfide bond terminates the FRET process. This explains the presence of blue emission from the cells even after the H₂O₂ treatment.

Flow cytometry experiments were carried out to further confirm the applicability of FLB₂SSCou for the intracellular

imaging of thiols and H₂O₂. We performed the same process of treatment to the cells before harvesting them for flow cytometry analysis. The analysis was performed with the brilliant violet 421 (BV421) channel and FITC channel, and the intensity of these measurements was then compared with blank cells, i.e. cells without the treatment of any agent (Figure 7G). Similar to the fluorescence images, a large percentage of the cells treated with FLB₂SSCou (10 μM) and β-CD (20 μM) showed emission signals from the BV421 channel accompanied by weak emission signals from the FITC channel (Figure 7H). It was observed that 19.75% of the cell population occupies the first quadrant of the dot plot, which are much higher than the cell population (0.01%) on the first quadrant in the control group (Figure 7G).

The same flow cytometry experiment was also performed on FLB₂SSCou-treated cells with the post-treatment of H₂O₂. From the dot plot (Figure 7I), it was observed that the cell population in the first quadrant (2.88%) greatly reduced, while having significant population increase in the second quadrant (93.98%). This set of cells have the largest population in the second quadrant as compared to other two cell groups, indicating that the post-treatment of H₂O₂ indeed turns on the green emission of internalized FLB₂SSCou measured by the FITC channel. When comparing the FITC signals from the one-dimensional histogram plots (Figure S4 in ESI), this group of cells show the highest FITC signal. Similar to the fluorescence microscopy images, we did not observe any significant decrease in the BV421 signal as compared to that of the cells treated with FLB₂SSCou and β-CD, once again confirming that the FRET process was terminated by the intracellular thiols.

Conclusions

In summary, we have developed a novel “turn-on” dual responsive fluorescence probe, FLB₂SSCou, for the detection of intracellular thiols and H₂O₂. In contrast to conventional “turn-on” fluorescence probes, FLB₂SSCou is capable of generating different emission responses when treated with thiols and H₂O₂. In the probe, a non-fluorescent diboronxanthene spiro isobenzofuran and a coumarin unit are bridged by a disulfide bond. The initial dark state of the probe is due to the PET process that occurs from the coumarin group into the isobenzofuran group. Upon treatment with thiols, reductive cleavage of the disulfide bond terminates this intramolecular PET process, thus initiating the emission from the coumarin unit. On the other hand, upon treatment with H₂O₂, the diboron xanthene spiro isobenzofuran group undergoes oxidation into a highly fluorescent fluorescein adduct, whereby the intramolecular PET process is converted into the intramolecular FRET process. A series of detection experiments have shown that the probe has the ability to sense thiols and H₂O₂ in a highly selective manner against over 20 amino acids.

In order to prove the intramolecular PET mechanism of FLB₂SSCou, the TD-DFT calculations have been carried out. A different distribution of the electron density between the ground state (S₀) and the first excited state (S₁) has been

observed, since the emission process is a result of the electronic relaxation from S_1 to S_0 . Moreover, the transition to the first excited state is a forbidden transition process ($f = 0.0000$), and instead, the first allowed transition is to the second excited state ($S_0 \rightarrow S_2$, $f = 0.6912$), where there is no redistribution of the electron density. Thus, it has been confirmed that the PET process occurs during a process where the electron first gains its energy to excite into the S_2 state followed by transferring into the S_1 state, since the direct excitation to the S_1 state is forbidden and there is inadequate energy for the spontaneous transfer.

Lastly, the *in vitro* intracellular imaging of thiols and H_2O_2 using FLB₂SSCou has been conducted. The fluorescence microscopy images show the presence of blue fluorescence within the intracellular environment of HeLa cells after the treatment with FLB₂SSCou, due to the interaction of FLB₂SSCou with intracellular thiols. On the other hand, the post-treatment of H_2O_2 on FLB₂SSCou-treated cells exhibits the enhancement in green fluorescence as compared to the cells without this post-treatment, indicating that exogenous H_2O_2 could induce a "turn-on" effect on the probe even in the intracellular environment. These results have been further supported by flow cytometry experiments, confirming the reproducibility of the probe for the detection and imaging of intracellular thiols and H_2O_2 . All in all, this work has successfully demonstrated the synthesis and applications of a dual responsive fluorescence probe for the simultaneous detection of thiols and H_2O_2 . The present research might inspire further development of "turn-on" fluorescence probes having multiple responsive properties.

Experimental section

General. All chemicals, reagents and solvents were used upon obtained from commercial sources without further purifications. Unless otherwise stated, the purification of compounds by flash chromatography was performed using Merck Geduran® Si 60 silica gel with particle sizes from 40 to 63 μm . Column was stacked with the slurry mixture of the silica gel and the eluting solvent. All ^1H NMR and ^{13}C NMR measurements were performed on a Bruker AMX AV400 MHz spectrophotometer at ambient temperature. ^1H two-dimension correlation spectroscopy (COSY) spectrum of FLB₂SSCou was measured with a Bruker AVIII 400 MHz NMR BBFO₂ probe spectrophotometer at ambient temperature. Signals from ^1H NMR spectra were reported as chemical shift in parts per million (ppm) calibrated using either deuterated solvent (7.26 ppm for CDCl_3 and 2.54 ppm for $\text{DMSO-}d_6$) or downfield from tetramethylsilane (0.00 ppm). Numbers of equivalent resonance protons are reported as nH and multiplicities are recorded as s (singlet), d (doublet), t (triplet), q (quartet), dd (doublet of doublet), ddd (doublet of doublet of doublet) and m (multiplet). Corresponding coupling constants (J value) for these multiplicities are reported in Hz. Signals from ^{13}C NMR spectra were reported as chemical shift in parts per million (ppm) calibrated using deuterated solvent (7.26 ppm for CDCl_3 and 2.54 ppm for $\text{DMSO-}d_6$). Fourier transform

infrared spectroscopy (FTIR) measurements were performed on a SHIMADZU IR Prestige-21 spectrophotometer. Melting points of solid compounds were recorded on an OptiMelt Automated Melting point instrument. High-resolution mass spectrometry (HRMS) was performed on a Waters Q-tof Premier MS. The UV-Vis spectroscopy studies for all optically active compounds were performed using a SHIMADZU UV-3600 UV-VIS-NIR spectrophotometer with a 10-mm-by-10-mm 1.4 mL quartz cuvette. Fluorescence emission spectra were recorded on a Varian Cary Eclipse fluorescence spectrophotometer equipped with water circulated temperature controller. Except for time-dependent fluorescence spectroscopy analysis, all fluorescence studies were carried out at 37°C using a 10-mm-by-10-mm 1.4 mL fluorescence cuvette. Time-dependent fluorescence spectroscopy analysis was performed with a 10-mm-by-10-mm 3.5 mL fluorescence cuvette. Unless otherwise stated, all UV-Vis and fluorescence spectroscopy experiments were performed in 0.1 X phosphate buffered saline (PBS). Spectroscopic studies in acidic conditions were conducted by dispersing the fluorophores in 0.1 M acetate buffer solution (pH 5.5).

HeLa cells used in this work were obtained from ATCC. Cells were maintained in a humidified CO_2 (5%) incubator and proliferated in Dulbecco's Modified Eagle Medium (DMEM) supplement with 10% fetal bovine serum and 1% penicillin streptomycin. Confocal microscopy experiments were conducted on a confocal microscope (Leica TCS SP5, 40 \times oil objective). Absorbance for the MTT cytotoxicity assay was measured with an Infinite 200 PRO multimode reader. Flow cytometry experiments were performed on a BD LSRFortessa™ X-20 cell analyzer.

7-(Diethylamino)-3-nitro-2H-chromen-2-one (1). The synthesis of compound **1** was performed based on a reported procedure.⁸⁴ Briefly, to a 50 mL flask containing *n*-butanol (20 mL) was added with 4-diethylaminosalicylaldehyde (0.97 g, 5.0 mmol), methyl 2-nitroacetate (502 μL , 5.15 mmol), piperidine (100 μL) and glacial acetic acid (2.5 mL). The mixture was heated to 110 °C under stirring condition for 18 h. The resulting dark brown solution was cooled down under ice bath when orange crystals were formed in the reaction mixture. The crystals were isolated by filtration and washed three times with ice cold *n*-butanol before drying under *vacuo* to afford **1** as a red-orange crystal (0.37 g, 28%). M.P.: 198.6–199.3°C. FTIR $\bar{\nu}/\text{cm}^{-1}$: 2980.02, 2935.66, 1743.65, 1631.78, 1591.27, 1544.98, 1477.47, 1427.32, 1327.03, 1188.15, 823.60, 767.67. ^1H NMR (400 MHz, CDCl_3): δ 8.72 (s, 1H), 7.44 (d, $J = 9.08$ Hz, 1H), 6.70 (dd, $J = 9.09$ & 2.37 Hz, 1H), 6.48 (d, $J = 2.22$ Hz, 1H), 3.50 (q, $J = 7.16$ Hz, 4H), 1.27 (t, $J = 7.16$ Hz, 6H). ^{13}C NMR (400 MHz, CHCl_3): δ 158.90, 154.69, 153.60, 143.47, 132.69, 127.03, 111.26, 106.35, 96.96, 45.66, 12.57. HRMS ($\text{H}_2\text{O}/\text{MeOH}$): m/z : calcd: 263.1032, found: 263.1038 [$\text{M}+\text{H}$]⁺.

3-Amino-7-(diethylamino)-2H-chromen-2-one (2). Compound **2** was synthesized based on a reported procedure.⁸⁵ To 25 mL flask containing 37% HCl (5 mL) was added with stannous chloride (1.35 g, 7.12 mmol) under stirring condition. Thereafter, compound **1** (0.25 g, 0.95 mmol) was added slowly

into the stirring solution and the resulting mixture was stirred for 4 h before pouring it into crushed ice (~20 g) with aqueous NaOH (5 M) in an ice bath. The resulting suspension was saturated with NaCl before extracting three times with diethyl ether. The organic layer was then washed with brine and dried over Na₂SO₄ before the solvent was removed under pressure to afford **2** as an orange solid (0.17 g, 77%). M.P.: 89.6–90.3°C. FTIR $\bar{\nu}/\text{cm}^{-1}$: 3400.50, 3338.78, 2970.38, 1695.43, 1624.06, 1591.27, 1523.76, 1134.14, 813.96, 798.53. ¹H NMR (400 MHz, CDCl₃): δ 7.11 (d, J = 8.68 Hz, 1H), 6.70 (s, 1H), 6.57 (dd, J = 8.69 & 2.51 Hz, 1H), 6.53 (d, J = 2.44 Hz, 1H), 3.37 (q, J = 7.08 Hz, 4H), 1.18 (t, J = 7.07 Hz, 6H). ¹³C NMR (400 MHz, CHCl₃): δ 160.33, 151.63, 147.50, 127.52, 125.95, 114.46, 109.68, 109.33, 98.03, 44.64, 12.50. HRMS (H₂O/MeOH): m/z : calcd: 233.1290, found: 233.1296 [M+H]⁺.

3-(Pyridin-2-ylidisulfanyl)propanoic acid (3). Compound **3** was synthesized based on a reported procedure.⁸⁶ To a stirring solution of 2,2'-dipyridyl disulfide (3.75 g, 17 mmol) in ethanol (10 mL) was added with acetic acid (0.4 mL). Thereafter, 3-mercaptopropionic acid (0.90 g, 8.47 mmol) in ethanol (5 mL) was dropwise added into the above solution, and the solution turned yellow gradually. The mixture was stirred for 20 h before ethanol was removed by rotary evaporation. The resulting yellow syrup was dissolved in CH₂Cl₂/ethanol (3:2, 10 mL) and loaded into a neutral alumina column, equilibrated with CH₂Cl₂/ethanol (3:2). The column was flushed with CH₂Cl₂/ethanol (3:2) until the yellow fraction was completely eluted out of the column. Thereafter, the column was flushed with CH₂Cl₂/ethanol (3:2) containing 4% acetic acid to elute the target product out of the column. The solvent was removed by rotary evaporation, and the remaining liquid was re-dissolved in CH₂Cl₂ and washed three times with water to remove acetic acid completely. The organic layer was washed with brine and dried over Na₂SO₄ before the solvent was removed by rotary evaporation. Finally, the residue was dried under *vacuo* to afford **3** as a white solid (1.42 g, 78%). M.P.: 61.2–62.6°C. FTIR $\bar{\nu}/\text{cm}^{-1}$: 3300–2400 (Broad), 2912.51, 1728.22, 1583.56, 1446.61, 1423.47, 1188.15, 1002.98, 765.74, 715.59. ¹H NMR (400 MHz, CDCl₃): δ 10.21 (broad s, 1H), 8.47 (m, 1H), 7.66 (m, 2H), 7.13 (ddd, J = 6.58 & 4.85 & 1.85 Hz, 1H), 3.04 (t, J = 6.95 Hz, 2H), 2.79 (t, J = 6.94, 2H). ¹³C NMR (400 MHz, CHCl₃): δ 176.16, 159.53, 149.44, 137.65, 121.27, 120.50, 34.04, 33.74. HRMS (H₂O/MeOH): m/z : calcd: 216.0157, found: 216.0153 [M+H]⁺.

N-(7-(Diethylamino)-2-oxo-2H-chromen-3-yl)-3-(pyridin-2-ylidisulfanyl)propanamide (4). To a stirring solution of compound **3** (0.24 g, 1.10 mmol) in THF (5 mL) was added with dicyclohexyl carbodiimide (0.23 g, 1.10 mmol) and N-hydroxysuccinimide (0.12 g, 1.07 mmol). The reaction was stirred for 2 h with the formation of white precipitate. Compound **2** (0.23 g, 1.00 mmol) was then added, and the resulting solution was refluxed for 24 h. The solid was removed by filtration, and the filtrate was concentrated by rotary evaporation. The obtained residual was purified by column chromatography eluted with 1:1 hexane/ethyl acetate to afford **4** as a yellow solid (0.16 g, 37%). M.P.: 130.8–131.9°C. FTIR $\bar{\nu}/\text{cm}^{-1}$: 3338.78, 2972.31, 2929.87, 1699.29, 1668.43,

1627.92, 1539.20, 1444.68, 1261.45, 1192.01, 1132.21, 763.81. ¹H NMR (400 MHz, CDCl₃): δ 8.59 (s, 1H), 8.54 (d, J = 4.83 Hz, 1H), 8.15 (s, 1H), 7.63 (m, 2H), 7.11 (m, 1H), 6.62 (dd, J = 8.81 & 2.46 Hz, 1H), 6.50 (d, J = 2.39 Hz, 1H), 3.40 (q, J = 7.10 Hz, 4H), 3.17 (t, J = 6.71 Hz, 2H), 2.85 (t, J = 6.75 Hz, 2H), 1.20 (t, J = 7.07 Hz, 6H). ¹³C NMR (400 MHz, CHCl₃): δ 169.74, 159.57, 152.83, 150.05, 149.59, 137.09, 128.81, 126.23, 122.64, 121.08, 120.27, 118.83, 109.75, 108.30, 105.76, 97.48, 44.85, 36.85, 34.59, 12.57. HRMS (H₂O/MeOH): m/z : calcd: 430.1259, found: 430.1249 [M+H]⁺.

3-((2-Aminoethyl)disulfanyl)-N-(7-(diethylamino)-2-oxo-2H-chromen-3-yl)propanamide HCl salt (5). In a 25 mL round bottom flask was loaded with compound **4** (0.22 g, 0.50 mmol) and acetic acid (30 μ L) in methanol (5 mL). The stirring solution was then added with mercaptoethanamine hydrochloride (0.05 g, 0.48 mmol). The reaction was allowed to react for 24 h and then the solvent was removed by rotary evaporation. The residue was re-dissolved in a small amount of methanol, which was poured into diethyl ether (100 mL) to induce the precipitation. The solid was isolated by filtration and then re-dissolved in a small amount of methanol before re-precipitating in diethyl ether (100 mL). The process was repeated for two more times until the supernatant turned colorless after the precipitation. The resulting yellow solid was dried under *vacuo* to afford compound **5** (0.15 g, 67%). FTIR $\bar{\nu}/\text{cm}^{-1}$: 3327.21, 2970.38, 1734.01, 1707.00, 1670.35, 1602.85, 1535.34, 1411.89, 1261.45, 1130.29, 823.60, 763.81. ¹H NMR (400 MHz, DMSO-*d*₆): δ 9.64 (s, 1H), 8.45 (s, 1H), 8.30 (broad s, 1H), 7.46 (d, J = 8.80 Hz, 1H), 6.73 (dd, J = 9.0 & 2.20 Hz, 1H), 6.56 (d, J = 8.81 & 2.0 Hz, 1H), 3.44 (q, J = 6.80 Hz, 7.5H, overlapped with HDO), 3.13 (t, J = 6.40 Hz, 2H), 3.04 (t, J = 6.00 Hz, 4H), 2.90 (t, J = 7.20 Hz, 2H), 1.15 (t, J = 6.80 Hz, 6H). ¹³C NMR (400 MHz, DMSO): δ 170.68, 158.69, 153.17, 149.68, 129.25, 128.22, 118.95, 109.91, 107.88, 97.08, 44.45, 38.20, 36.07, 34.39, 34.02, 12.79. HRMS (H₂O/MeOH): m/z : calcd: 408.1416, found: 408.1432 [M-Cl]⁺.

3',6'-Dibromo-3-oxo-3H-spiro[isobenzofuran-1,9'-xanthene]-6-carboxylic acid (6). 3-Bromophenol (27.64 g, 159.80 mmol) and benzene-1,2,4-tricarboxylic acid (16.80 g, 79.90 mmol) were charged into a 3-neck flask equipped with a reflux condenser. Gaseous exchange was then performed, cycling between N₂ and *vacuo* for at least three times. Thereafter, methanesulfonic acid (60 mL) was injected into the flask and the reaction was heated at 140°C for 72 h. The reaction was cooled down to ambient temperature before pouring it into ice water (400 mL). The precipitate was then collected by filtration and dried in *vacuo*. The resulting brown solid was dissolved in acetic anhydride/pyridine mixture (3:1, 160 mL) to induce the precipitation. The white precipitate was isolated and the red filtrate was discarded. The white precipitate was washed with acetic anhydride/pyridine mixture (2:1, 60 mL) for six times to ensure complete removal of any pink stain. The resulting white solid was then washed with aqueous HCl (1 M, 100 mL) for three times followed by washing with water for three times. The solid was dried under *vacuo* to afford compound **6** as a brownish white solid (9.14 g, 23%). M.P.: 89.6–90.3°C (decomposition temperature). FTIR $\bar{\nu}/\text{cm}^{-1}$: 3300-

2400 (broad), 2974.23, 2766.80, 1720.50, 1593.20, 1479.40, 1230.58, 1074.35, 921.97, 817.82, 754.17. ^1H NMR (400 MHz, DMSO- d_6): δ 8.61 (s, 1H), 8.30 (dd, J = 8.01, 1.26, 1H), 8.21 (d, J = 7.97 Hz, 1H), 7.89 (s, 1H), 7.73 (d, J = 1.90 Hz, 2H), 7.36 (dd, J = 8.51 & 1.92 Hz, 2H), 6.91 (d, J = 8.52 Hz, 2H). ^{13}C NMR (400 MHz, DMSO- d_6): δ 168.01, 166.40, 152.65, 151.20, 149.79, 138.25, 136.96, 131.95, 130.49, 129.03, 128.14, 126.17, 125.17, 124.49, 81.26. HRMS ($\text{H}_2\text{O}/\text{MeOH}$): m/z : calcd: 500.8973 found: 500.8986 $[\text{M}+\text{H}]^+$.

3-Oxo-3',6'-bis(4,4,5,5-tetramethyl-1,3,2-dioxaborolan-2-yl)-3H-spiro[isobenzofuran-1,9'-xanthene]-6-carboxylic acid (7). To a oven-dried 3-neck flask was charged with compound **6** (2.00 g, 4.00 mmol), [1,1'-bis(diphenylphosphino)ferrocene]dichloro palladium (II) dichloromethane adduct (0.98 g, 1.20 mmol), potassium acetate (3.94 g, 40.10 mmol) and bis(pinacolato)diboron (4.00 g, 15.80 mmol). The flask was evacuated before back filling with N_2 gas. The process was repeated twice before anhydrous DMF (50 mL) was injected into the flask. The mixture was stirred at room temperature for 5 min, and then stirred at 80°C for 12 h. Thereafter, DMF was distilled off under reduced pressure and the resulting black mass was suspended in ethyl acetate (~30 mL). The mixture was washed three times with aqueous HCl (0.1 M) and once with water. The organic layer was subjected to filtration to remove any insoluble solid, and the filtrate was washed with brine and dried over Na_2SO_4 to remove any trace of water. The solvent was then removed by rotary evaporation. The obtained crude product was purified by flash column chromatography equilibrated with hexane, eluting with hexane/ethyl acetate mixture (gradient from 50:50 to 10:90). The solvent was removed under pressure to obtain brown slurry, and the slurry was added with Et_2O . The solid was then obtained by vacuum filtration and washed with Et_2O to afford compound **7** as a white solid (0.52 g, 22%). M.P.: $265.0\text{--}265.8^\circ\text{C}$ (decomposition temperature). FTIR $\bar{\nu}/\text{cm}^{-1}$: 3600-2400 (broad), 3145.90, 2980.02, 1737.86, 1406.11, 1359.82, 1143.79, 1087.85, 974.05, 854.45, 825.53, 688.59. ^1H NMR (400 MHz, DMSO- d_6): δ 8.28 (dd, J = 8.04 & 1.05 Hz, 1H), 8.22 (d, J = 8.02 Hz, 1H), 7.71 (s, 1H), 7.65 (s, 2H), 7.44 (d, J = 7.84 Hz, 2H), 6.98 (d, J = 7.85 Hz, 2H), 1.35 (s, 24H). ^{13}C NMR (400 MHz, DMSO- d_6): δ 168.31, 166.30, 153.62, 150.29, 138.24, 131.79, 130.00, 128.56, 128.02, 126.18, 124.78, 123.31, 121.15, 84.68, 81.64, 25.08. HRMS ($\text{H}_2\text{O}/\text{MeOH}$): m/z : calcd: 596.2504, found: 596.2534 $[\text{M}+\text{H}]^+$.

N-(2-((3-(7-(Diethylamino)-2-oxo-2H-chromen-3-yl)amino)-3-oxopropyl)disulfanyl)ethyl)-3-oxo-3',6'-bis(4,4,5,5-tetramethyl-1,3,2-dioxaborolan-2-yl)-3H-spiro[isobenzofuran-1,9'-xanthene]-6-carboxamide (8) or FLB₂SSCou. To a stirring solution of compound **7** (0.14 g, 0.23 mmol) in THF (5 mL) was added with *N*-hydroxysuccinimide (0.03 g, 0.25 mmol) and dicyclohexylcarbodiimide (0.05 g, 0.25 mmol). The solution was stirred for 3 h when white precipitate of dicyclohexylurea was formed. Thereafter, compound **5** (0.10 g, 0.23 mmol) and Et_3N (70 μL , 0.50 mmol) were added to the above solution for refluxing overnight. The solvent was removed by rotary evaporation and the residue was purified by flash chromatography, eluting with ethyl acetate/hexane mixture

(1:1) to afford compound **8** as a yellow solid (30 mg, 13%). M.P.: $140.2\text{--}141.7^\circ\text{C}$. FTIR $\bar{\nu}/\text{cm}^{-1}$: 3313.71, 2976.16, 2926.01, 2908.65, 1772.58, 1676.14, 1654.92, 1608.63, 1560.41, 1533.41, 1508.33, 1406.11, 1357.89, 1141.86, 1087.85, 974.05, 854.47, 825.53, 692.44. ^1H NMR (400 MHz, CDCl_3): δ 8.38 (s, 1H), 8.09 (s, 2H), 8.02 (s, 1H), 7.72 (s, 2H), 7.54 (s, 1H), 7.40 (d, J = 7.84 Hz, 2H), 7.14 (d, J = 8.63 Hz, 1H), 6.82 (d, J = 7.75 Hz, 2H), 6.62-6.59 (m, 1H), 6.49 (s, 1H), 3.71 (q, J = 5.91 Hz, 2H), 3.45-3.38 (m, 4H), 3.00 (t, J = 6.56 Hz, 2H), 2.86 (t, J = 6.05 Hz, 2H), 2.76 (t, J = 6.55 Hz, 2H), 1.33 (s, 24H), 1.23 (t, J = 10.85 Hz, 6H). ^{13}C NMR (400 MHz, CDCl_3): δ 169.67, 168.81, 165.88, 159.55, 154.47, 152.76, 150.44, 149.65, 140.95, 129.49, 129.02, 128.71, 127.63, 126.83, 126.30, 125.57, 123.70, 122.66, 120.70, 118.42, 109.75, 108.00, 97.40, 84.25, 82.19, 44.78, 39.03, 37.88, 37.30, 33.92, 33.50, 24.83. HRMS ($\text{H}_2\text{O}/\text{MeOH}$): m/z : calcd: 972.3542, found: 972.3682 $[\text{M}+\text{H}]^+$.

Quantum yield measurements. Relative quantum yields of various compounds were measured by the following formula using fluorescein as the standard reference ($\Phi_{\text{std}} = 0.85$ in 1 N NaOH).⁸⁷

$$\Phi_{\text{sample}} = \Phi_{\text{std}} \frac{\int \text{Fl}_{\text{sample}} d\lambda}{\int \text{Fl}_{\text{std}} d\lambda} \frac{1 - 10^{-\text{Abs}_{\text{std}}}}{1 - 10^{-\text{Abs}_{\text{sample}}}}$$

where Φ represents the quantum yield, $\int \text{Fl} d\lambda$ represents the integrated area in fluorescence spectra, and Abs represents the absorbance at the λ_{max} of sample (sample) and standard (std).

Detection limit measurements. Detection limit measurements of FLB₂SSCou with respect to GSH and H_2O_2 were performed based on a reported procedure.²² The measurements were carried out by incubating the analyte (various concentrations) with the probe in PBS at 37°C overnight followed by measuring the emission spectra. The maximum emission intensities were plotted against the concentrations to obtain a linear plot, and the gradient (k) of the plot was then obtained. The maximum emission intensity of FLB₂SSCou was measured five times, and the standard deviation (σ) of these measurements was obtained. Lastly, detection limit was measured using the following formula.

$$\text{Detection Limit} = \frac{3\sigma}{k}$$

Computation studies. Theoretical calculations on various adducts were performed using the Gaussian 09 package. DFT optimizations of the adducts were performed using the basis set of B3LYP/6-31++G(d,p). Water as solvent was simulated with the polarizable continuum model (PCM) using the integral equation formalism variant (IEFPCM) during the calculation process. The optimized structures were used to proceed with the TD-DFT calculation using the same basis set and solvent simulation.

Confocal scanning microscopy experiments. HeLa cells were first seeded on a SPL 200350 coverglass-bottom dish at a seeding density of 2×10^5 cells (2 mL) per well. The cells were incubated overnight prior to the addition of FLB₂SSCou (10 μM) and β -CD (20 μM) solution. The cells were then incubated overnight with the samples followed by the removal of the medium. The cells were washed three times with PBS and finally added with fresh medium (2 mL). For the post-

ARTICLE

Journal Name

treatment with H₂O₂, H₂O₂ was added into the cells right after the medium replacement to achieve a concentration of 150 μM. All the cells were incubated at 37°C for another 20 min prior to washing the cells for 3 times with PBS and then fixing with 4% formaldehyde. The cells were washed once with PBS again before imaging.

Flow cytometry experiments. HeLa cells were first seeded on a 6-well plate at a seeding density of 2 × 10⁵ cells (2 mL) per well. The cells were incubated overnight prior to the addition of FLB₂SSCou (10 μM) and β-CD (20 μM) solution. The cells were then incubated with the samples overnight before the removal of the medium. The cells were washed three times with PBS and finally added with trypsin (500 μL) to induce cell detachment. Thereafter, fresh medium (500 μL) was added to quench off trypsin before harvesting the cells. The cells were isolated by low speed centrifugation (2000 rpm, 3 min), and the obtained cell pellets were washed two times with PBS and finally re-suspended in PBS (1 mL). For the post-treatment with H₂O₂, H₂O₂ was added into the cells right after the PBS suspension so as to achieve a concentration of 150 μM. All the cells were incubated at 37°C for another 45 min prior to flow cytometry experiments. Flow cytometry experiments were performed at the gated population of 10,000 events.

Acknowledgements

This work is supported by the National Research Foundation (NRF), Prime Minister's Office, Singapore under its NRF Fellowship (NRF2009NRF-RF001-015), and Campus for Research Excellence and Technological Enterprise (CREATE) Programme–Singapore Peking University Research Centre for a Sustainable Low-Carbon Future, as well as the NTU-A*Star Silicon Technologies Centre of Excellence under the program grant No. 112 351 0003.

Notes and References

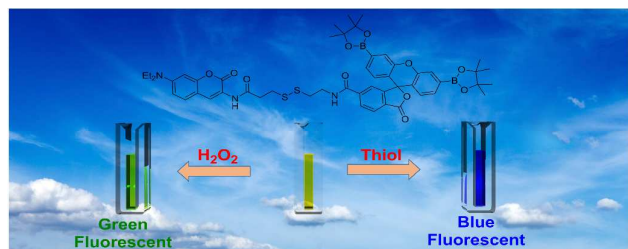
- Y. Yang, Q. Zhao, W. Feng and F. Li, *Chem. Rev.*, 2012, **113**, 192-270.
- Y. Zhou, J. F. Zhang and J. Yoon, *Chem. Rev.*, 2014, **114**, 5511-5571.
- J. Chan, S. C. Dodani and C. J. Chang, *Nat. Chem.*, 2012, **4**, 973-984.
- X. Chen, Y. Zhou, X. J. Peng and J. Yoon, *Chem. Soc. Rev.*, 2010, **39**, 2120-2135.
- M. E. Jun, B. Roy and K. H. Ahn, *Chem. Commun.*, 2011, **47**, 7583-7601.
- D. Kim, H. G. Ryu and K. H. Ahn, *Org. Biomol. Chem.*, 2014, **12**, 4550-4566.
- S. Ziegler, V. Pries, C. Hedberg and H. Waldmann, *Angew. Chem. Int. Ed.*, 2013, **52**, 2744-2792.
- M. H. Lee, J. S. Kim and J. L. Sessler, *Chem. Soc. Rev.*, 2015, DOI: 10.1039/C4CS00280F.
- K. P. Carter, A. M. Young and A. E. Palmer, *Chem. Rev.*, 2014, **114**, 4564-4601.
- J. Wu, W. Liu, J. Ge, H. Zhang and P. Wang, *Chem. Soc. Rev.*, 2011, **40**, 3483-3495.
- R. W. Sinkeldam, N. J. Greco and Y. Tor, *Chem. Rev.*, 2010, **110**, 2579-2619.
- M. Schäferling, *Angew. Chem. Int. Ed.*, 2012, **51**, 3532-3554.
- H. Kobayashi, M. Ogawa, R. Alford, P. L. Choyke and Y. Urano, *Chem. Rev.*, 2009, **110**, 2620-2640.
- X. Li, X. Gao, W. Shi and H. Ma, *Chem. Rev.*, 2013, **114**, 590-659.
- J. Liu, Y. Q. Sun, Y. Y. Huo, H. X. Zhang, L. F. Wang, P. Zhang, D. Song, Y. W. Shi and W. Guo, *J. Am. Chem. Soc.*, 2014, **136**, 574-577.
- H. S. Jung, X. Q. Chen, J. S. Kim and J. Yoon, *Chem. Soc. Rev.*, 2013, **42**, 6019-6031.
- H. Guo, Y. Jing, X. Yuan, S. Ji, J. Zhao, X. Li and Y. Kan, *Org. Biomol. Chem.*, 2011, **9**, 3844-3853.
- S. Sreejith, K. P. Divya and A. Ajayaghosh, *Angew. Chem. Int. Ed.*, 2008, **47**, 7883-7887.
- S.-T. Huang, K.-N. Ting and K.-L. Wang, *Anal. Chim. Acta*, 2008, **620**, 120-126.
- L. Yi, H. Y. Li, L. Sun, L. L. Liu, C. H. Zhang and Z. Xi, *Angew. Chem. Int. Ed.*, 2009, **48**, 4034-4037.
- B. Tang, Y. Xing, P. Li, N. Zhang, F. Yu and G. Yang, *J. Am. Chem. Soc.*, 2007, **129**, 11666-11667.
- L. L. Long, L. P. Zhou, L. Wang, S. C. Meng, A. H. Gong, F. Y. Du and C. Zhang, *Org. Biomol. Chem.*, 2013, **11**, 8214-8220.
- G.-J. Kim, K. Lee, H. Kwon and H.-J. Kim, *Org. Lett.*, 2011, **13**, 2799-2801.
- T. Zou, C. T. Lum, S. S.-Y. Chui and C.-M. Che, *Angew. Chem. Int. Ed.*, 2013, **52**, 2930-2933.
- L.-Y. Niu, Y.-S. Guan, Y.-Z. Chen, L.-Z. Wu, C.-H. Tung and Q.-Z. Yang, *J. Am. Chem. Soc.*, 2012, **134**, 18928-18931.
- F. Wang, Z. Guo, X. Li, X. Li and C. Zhao, *Chem. Eur. J.*, 2014, **20**, 11471-11478.
- H. Zhang, C. Zhang, R. Liu, L. Yi and H. Sun, *Chem. Commun.*, 2015, **51**, 2029-2032.
- A. R. Sarkar, C. H. Heo, E. Kim, H. W. Lee, H. Singh, J. J. Kim, H. Kang, C. Kang and H. M. Kim, *Chem. Commun.*, 2015, **51**, 2407-2410.
- N. Sato, S. Iwata, K. Nakamura, T. Hori, K. Mori and J. Yodoi, *J. Immunol.*, 1995, **154**, 3194-3203.
- S. Zhang, C. N. Ong and H. M. Shen, *Cancer Lett.*, 2004, **208**, 143-153.
- C. Y. Ang, S. Y. Tan and Y. Zhao, *Org. Biomol. Chem.*, 2014, **12**, 4776-4806.
- R. H. Schirmer, J. G. Muller and R. L. Krauthsiegel, *Angew. Chem. Int. Ed. Engl.*, 1995, **34**, 141-154.
- S. Seshadri, A. Beiser, J. Selhub, P. F. Jacques, I. H. Rosenberg, R. B. D'Agostino, P. W. F. Wilson and P. A. Wolf, *N. Engl. J. Med.*, 2002, **346**, 476-483.
- L. A. Herzenberg, S. C. De Rosa, J. G. Dubs, M. Roederer, M. T. Anderson, S. W. Ela, S. C. Deresinski and L. A. Herzenberg, *Proc. Natl. Acad. Sci. U.S.A.*, 1997, **94**, 1967-1972.
- K. Yuan, Y. Liu, H.-N. Chen, L. Zhang, J. Lan, W. Gao, Q. Dou, E. C. Nice and C. Huang, *Proteomics*, 2015, **15**, 287-299.
- C. R. Schlegel, M. L. Georgiou, M. B. Misterek, S. Stocker, E. R. Chater, C. E. Munro, O. E. Pardo, M. J. Seckl and A. P. Costa-Pereira, *Cell Death Dis.*, 2015, **6**, e1671.
- G. K. Balendiran, R. Dabur and D. Fraser, *Cell Biochem. Funct.*, 2004, **22**, 343-352.
- H. Aziz, R. Gaafar, A. Bahnassy and A. Helal, *Lung Cancer*, 2012, **77**, Supplement 1, S21.

39. C. S. Morrow, C. Pecklak-Scott, B. Bishwokarma, T. E. Kute, P. K. Smitherman and A. J. Townsend, *Mol. Pharmacol.*, 2006, **69**, 1499-1505.
40. N. Shao, J. Jin, H. Wang, J. Zheng, R. Yang, W. Chan and Z. Abliz, *J. Am. Chem. Soc.*, 2009, **132**, 725-736.
41. K. D. Tew, *Pigment Cell Melanoma Res.*, 2011, **24**, 1078-1079.
42. R. Hong, G. Han, J. M. Fernández, B.-j. Kim, N. S. Forbes and V. M. Rotello, *J. Am. Chem. Soc.*, 2006, **128**, 1078-1079.
43. X. Wang, X. Cai, J. Hu, N. Shao, F. Wang, Q. Zhang, J. Xiao and Y. Cheng, *J. Am. Chem. Soc.*, 2013, **135**, 9805-9810.
44. H. Kim, S. Kim, C. Park, H. Lee, H. J. Park and C. Kim, *Adv. Mater.*, 2010, **22**, 4280-4283.
45. Q. Zhang, F. Liu, K. T. Nguyen, X. Ma, X. J. Wang, B. G. Xing and Y. L. Zhao, *Adv. Funct. Mater.*, 2012, **22**, 5144-5156.
46. J. Zhang, Z.-F. Yuan, Y. Wang, W.-H. Chen, G.-F. Luo, S.-X. Cheng, R.-X. Zhuo and X.-Z. Zhang, *J. Am. Chem. Soc.*, 2013, **135**, 5068-5073.
47. Q. Zhang, X. Wang, P.-Z. Li, K. T. Nguyen, X.-J. Wang, Z. Luo, H. Zhang, N. S. Tan and Y. Zhao, *Adv. Funct. Mater.*, 2013, **24**, 2450-2461.
48. S. Y. Tan, C. Y. Ang, P. Li, Q. M. Yap and Y. Zhao, *Chem. Eur. J.*, 2014, **20**, 11276-11282.
49. X. Ma, K. T. Nguyen, P. Borah, C. Y. Ang and Y. Zhao, *Adv. Healthc. Mater.*, 2012, **1**, 690-697.
50. S. Y. Tan, C. Y. Ang, Z. Luo, P. Li, K. T. Nguyen and Y. Zhao, *Chem. Eur. J.*, 2015, **21**, 6123-6131.
51. C. Nathan and A. Cunningham-Bussell, *Nat. Rev. Immunol.*, 2013, **13**, 349-361.
52. T. Finkel, *Curr. Opin. Cell Biol.*, 2003, **15**, 247-254.
53. S. G. Rhee, *Science*, 2006, **312**, 1882-1883.
54. H. Yagi, J. Tan and R. S. Tuan, *J. Cell. Biochem.*, 2013, **114**, 1163-1173.
55. E. W. Miller, O. Tulyathan, E. Y. Isacoff and C. J. Chang, *Nat. Chem. Biol.*, 2007, **3**, 263-267.
56. T. P. Sztatowski and C. F. Nathan, *Cancer Res.*, 1991, **51**, 794-798.
57. R. S. Sohal, H.-H. Ku, S. Agarwal, M. J. Forster and H. Lal, *Mech. Ageing Dev.*, 1994, **74**, 121-133.
58. L. Park, P. Zhou, R. Pitstick, C. Capone, J. Anrather, E. H. Norris, L. Younkin, S. Younkin, G. Carlson, B. S. McEwen and C. Iadecola, *Proc. Natl. Acad. Sci. U.S.A.*, 2008, **105**, 1347-1352.
59. A. M. Shah and K. M. Channon, *Heart*, 2004, **90**, 486-487.
60. G. C. Van de Bittner, E. A. Dubikovskaya, C. R. Bertozzi and C. J. Chang, *Proc. Natl. Acad. Sci. U.S.A.*, 2010, **107**, 21316-21321.
61. S. D. Lim, C. Sun, J. D. Lambeth, F. Marshall, M. Amin, L. Chung, J. A. Petros and R. S. Arnold, *Prostate*, 2005, **62**, 200-207.
62. A. R. Lippert, G. C. Van de Bittner and C. J. Chang, *Acc. Chem. Res.*, 2011, **44**, 793-804.
63. J. Fan, M. Hu, P. Zhan and X. Peng, *Chem. Soc. Rev.*, 2013, **42**, 29-43.
64. A. E. Albers, V. S. Okreglak and C. J. Chang, *J. Am. Chem. Soc.*, 2006, **128**, 9640-9641.
65. H. Takakusa, K. Kikuchi, Y. Urano, H. Kojima and T. Nagano, *Chem. Eur. J.*, 2003, **9**, 1479-1485.
66. G. Zheng, Y.-M. Guo and W.-H. Li, *J. Am. Chem. Soc.*, 2007, **129**, 10616-10617.
67. D. Srikun, A. E. Albers and C. J. Chang, *Chem. Sci.*, 2011, **2**, 1156-1165.
68. M. C. Y. Chang, A. Pralle, E. Y. Isacoff and C. J. Chang, *J. Am. Chem. Soc.*, 2004, **126**, 15392-15393.
69. E. W. Miller, A. E. Albers, A. Pralle, E. Y. Isacoff and C. J. Chang, *J. Am. Chem. Soc.*, 2005, **127**, 16652-16659.
70. D. Srikun, E. W. Miller, D. W. Domaille and C. J. Chang, *J. Am. Chem. Soc.*, 2008, **130**, 4596-4597.
71. A. E. Albers, B. C. Dickinson, E. W. Miller and C. J. Chang, *Bioorg. Med. Chem. Lett.*, 2008, **18**, 5948-5950.
72. D. Srikun, A. E. Albers, C. I. Nam, A. T. Iavarone and C. J. Chang, *J. Am. Chem. Soc.*, 2010, **132**, 4455-4465.
73. B. C. Dickinson, C. Huynh and C. J. Chang, *J. Am. Chem. Soc.*, 2010, **132**, 5906-5915.
74. A. R. Lippert, T. Gschneidner and C. J. Chang, *Chem. Commun.*, 2010, **46**, 7510-7512.
75. C. Chung, D. Srikun, C. S. Lim, C. J. Chang and B. R. Cho, *Chem. Commun.*, 2011, **47**, 9618-9620.
76. Bryan C. Dickinson, Y. Tang, Z. Chang and Christopher J. Chang, *Chem. Biol.*, 2011, **18**, 943-948.
77. V. Carroll, B. W. Michel, J. Blecha, H. VanBrocklin, K. Keshari, D. Wilson and C. J. Chang, *J. Am. Chem. Soc.*, 2014, **136**, 14742-14745.
78. M. J. Frisch, G. W. Trucks, H. B. Schlegel, G. E. Scuseria, M. A. Robb, J. R. Cheeseman, G. Scalmani, V. Barone, B. Mennucci, G. A. Petersson, H. Nakatsuji, M. Caricato, X. Li, H. P. Hratchian, A. F. Izmaylov, J. Bloino, G. Zheng, J. L. Sonnenberg, M. Hada, M. Ehara, K. Toyota, R. Fukuda, J. Hasegawa, M. Ishida, T. Nakajima, Y. Honda, O. Kitao, H. Nakai, T. Vreven, J. A., Jr. Montgomery, J. E. Peralta, F. Ogliaro, M. Bearpark, J. J. Heyd, E. Brothers, K. N. Kudin, V. N. Staroverov, R. Kobayashi, J. Normand, K. Raghavachari, A. Rendell, J. C. Burant, S. S. Iyengar, J. Tomasi, M. Cossi, N. Rega, J. M. Millam, M. Klene, J. E. Knox, J. B. Cross, V. Bakken, C. Adamo, J. Jaramillo, R. Gomperts, R. E. Stratmann, O. Yazyev, A. J. Austin, R. Cammi, C. Pomelli, J. W. Ochterski, R. L. Martin, K. Morokuma, V. G. Zakrzewski, G. A. Voth, P. Salvador, J. J. Dannenberg, S. Dapprich, A. D. Daniels, Ö. Farkas, J. B. Foresman, J. V. Ortiz, J. Cioslowski and D. J. Fox, Gaussian 09, Revision A.02, Gaussian, Inc., Wallingford CT, 2009.
79. V. R. Batistela, J. da Costa Cedran, H. P. Moisés de Oliveira, I. S. Scarmínio, L. T. Ueno, A. Eduardo da Hora Machado and N. Hioka, *Dyes Pigments*, 2010, **86**, 15-24.
80. D. P. Murale, H. Kim, W. S. Choi and D. G. Churchill, *RSC Adv.*, 2014, **4**, 5289-5292.
81. M. Ali, P. Dutta and S. Pandey, *J. Phys. Chem. B*, 2010, **114**, 15042-15051.
82. B. Valeur, *Molecular Fluorescence: Principles and Applications*, Wiley-VCH, Weinheim, Germany, 2001.
83. Y. Kanaoka, *Angew. Chem. Int. Ed. Engl.*, 1977, **16**, 137-147.
84. Y. Zhou, K. Chu, H. Zhen, Y. Fang and C. Yao, *Spectrochim. Acta Mol. Biomol. Spectros.*, 2013, **106**, 197-202.
85. N. Gagey, M. Emond, P. Neveu, C. Benbrahim, B. Goetz, I. Aujard, J.-B. Baudin and L. Jullien, *Org. Lett.*, 2008, **10**, 2341-2344.
86. A. Janshoff, K.-P. S. Dancil, C. Steinem, D. P. Greiner, V. S. Y. Lin, C. Gurtner, K. Motesharei, M. J. Sailor and M. R. Ghadiri, *J. Am. Chem. Soc.*, 1998, **120**, 12108-12116.
87. T. Miura, Y. Urano, K. Tanaka, T. Nagano, K. Ohkubo and S. Fukuzumi, *J. Am. Chem. Soc.*, 2003, **125**, 8666-8671.

ARTICLE

Journal Name

TOC Figure



A dual responsive probe capable of generating two different responses upon reacting with thiols and H_2O_2 in a highly selective manner was developed.